Definition of wind vectors and movement of dusts in air

Tomoo AOYAMA[1], Yuji OBARA[1], Junko KAMBE[1]

Abstract

To discuss the movement of dusts in the air, we show a construction of wind fields, a separation approach of the convection-diffusion equation, and a modeling of a forest fire. They are tested in case of a forest fire in Namie town in 2017, where is radioactive contaminated area. ^{137}Cs dust is observed there, and the re-diffusion is found.

Keywords: wind interpolation, IDW, Kriging, vertical direction wind, radionuclides, re-diffusion, deposition, forest fire model, Gaussian-puff, back trajectory, dust transportation.

Introduction

The 4-dimensional (4D) wind field is an important data for environmental analysis. It drives the movements of compounds or dusts in airspace. Dusts are emitted and deposited and moved by events, gravity, and winds. They are solved as a convection-diffusion problem physically. If transported matters are dangerous; we should be concern with the diffusion in environment.

We discuss how to construct with the field derived from observations. The derivation is interpolation and/or extrapolation between discrete 2D towards continuous 3D as for the space. We do not make continuous expansion for time-axis, here. We set precision is 16 bits for 3D axis, and time axis is per 10 min. The field has not mesh structure.

We solve a transport problem by using the convection-diffusion equation, which is separated into convection and diffusion parts approximately. Deposition process of dusts is reduced to the terminal velocity of particles.

We see a forest fire at Mt. Jyuman in Namie town, Fukushima. The area is contaminated by radioactive nuclides of 0.24 ~ 2.85×10^5 Bq/m^2 on the ground [1]. The ^{137}Cs dust is observed at 3 points around the mountain, whose density is about 3 ~ 25 mBq/m^3. It is significant observations. Because nowadays, we are living in dusts of μBq/m^3 level. We believe it is the first re-diffusing event of radioactive nuclides in Japan. To understand the influences, we construct with a model of the forest fire.

1. Observation winds

The wind field is included in GPV (grid point value) also, but the mesh interval is 5.5 ~ 11 km and 1 ~ 3 h in the surface-field of MSM (meta-scale model; This is the maximum resolution model.) [2]. The vertical wind is sometimes none. Moreover, MSM-GPV data of a half-day are over 320 MB. On environmental researches, a period is 20 days at least. We adopt another approach to get a wind field.

Constructing a field, winds at many locations are required. The time interval is 10 min. If it is winds per 1h, details of transportation would not be clear. Even if GPV winds are self-consistent, that interpolated from 1 h winds does not give the details.

Speaking strictly; environmental events are often happened by turbulence during pulse winds. It requires instantaneous wind of 3 s. It is observed by JMA (Japan Meteorological Agency) [3]. Number of the data is less.

We estimate transportation events by using 10 min winds, which are published by AMDS (Automated Meteorological Data Acquisition System, JMA [4]) and DB of Monitoring information of environmental radioactivity level (Nuclear Regulation Authority, Japan) [5]. Some local governments observe the winds [6], and sometimes the data are released. Using some approaches, we get 32 kinds of wind data for 31×39 km zone in Fukushima, which are listed in Appendix 1.

2. Vector analysis of winds

2.1 Interpolation for the plane

Observations are done at discrete locations; they are converted to be continued by using interpolation and extrapolation; the both function is required. Hereafter simplify, the extrapolation is included to the interpolation.

For nth dimensional interpolation, an inverse distance weighting (IDW) approach is known [7]. The IDW is a Kriging approach [7], where adopted function must be

2018年1月31日受付　2018年2月5日受理
1) Edogawa Univercity Institute of Information Education

optimized to target phenomenon. The simplest expression is,

$\hat{}Val(\boldsymbol{x})=\{w_i(\boldsymbol{x})Val(x_i)\}\{w_i(\boldsymbol{x})\};$

$w_i(\boldsymbol{x})=Distance(\boldsymbol{x},x_i)^{-p},$ (1a)

$Distance(\boldsymbol{x},x_i)=\{(x-x_i)^2+(y-y_i)^2+....\}^{0.5},$

$\boldsymbol{x}=(x,y,z,...).$ (1b)

The $\hat{}Val(\boldsymbol{x})$ is an averaged (^) scalar-value at $\boldsymbol{x}$ position. Bold character is a vector.

The wind data are expressed by 3 elements of u-, v-, z-values; *i.e.*, (u,v,z). In meteorological field, the z-wind is written as w-wind. "p" is a parameter; $p=1$ is adopted normally. Thus; each element is interpolated as if it is a scalar independently. The interpolation has not conservation law. Therefore, we must introduce the law towards IDW; *i.e.*,

$(\partial/\partial x,\partial/\partial y,\partial/\partial z)(u,v,z)=div(u,v,z)=0,$ (2)

Eq.(2) equivalents that the air is non-compressive liquid and there is no emission in the field. Under the condition, a z-element of the wind is calculated by (u,v)-elements. This is a popular approach in the meteorological field.

We find that the wind speed is interpolated linearly. The reason is following: (1) The wind is arisen by the difference of atmospheric pressures. (2) The wind speed between two positions is gradually larger during the pressure is kept. However; Eq.(1a) has a weight of the inverse function, which is not acceptable.

There are many locations observed the wind. If we adopt a finite linear function, the slope depends on the distance. That means many kinds of linear functions are required; thus, we don't adopt the functions. We require a function that has no dependency for directions and can be continuous toward infinity, and it must be linear changes partially. Such a function is not existed; however, based on a restricted interval [0,10], a function can be defined approximately. The expression is;

$w_i(x)=exp\{-A(\boldsymbol{x}-x_i)^2\},$

$A=Ln(0.1)/dmax^2,\ A=-0.023025851.$ (3)

Where $dmax$ is the maximum distance [km] from the nearest observation point. In this paper, $dmax=10$ is set. "0.1" is that a contribution from 10 km point is set 1/10. Eq.(3) indicates that the interval of observation points must be located inner 10 km. *That is;* we select such a function instead of Kriging optimization one.

Σ of Eq.(1a) is whole observation points in original IDW. However, If $Val(\boldsymbol{x})$ is an element of vector, the operation should be restricted for near points, because of property of winds. We select winds of near 3 points; *i.e.*, a mesh structure like as the FEM (finite element method) is introduced.

The 3 closest points are chosen by the distance in case of a simple IDW. This is not suitable for wind interpolation. The points should be chosen to include a target point inside like as FEM mesh. We calculate 5 closest points and count their angle distribution sum around the target point, and adopt the minimum case. It gives locations near FEM mesh. However, it is not possible at whole case; especially the case is found outer of circumference line of observation points. The interpolation gives low precision in such a case.

2.2 Interpolation for z- and t-axis

Kondow's expression [8] is known for the wind speed along vertical direction. The expression requires the friction speed. Since original expression is non programmable, we rewrite Eq.(4) to 10 m window adopted on JMA standard, and Eq.(5) is got.

$V(z)=(u^*/\kappa)Ln(z/z_0),\ u^*=\kappa\{V(z)/Ln(z/z_0)\},$ (4)

$V(z)=\{Ln(z/z_0)/Ln(10/z_0)\}V(10),$ (5)

Where, $\{V(z),\ u^*,\ \kappa,\ z,\ z_0\}$ is {wind speed [m/s] at height z [m], friction speed [m/s], Karman's constant [no unit], vertical direction from the ground [m], aerodynamic roughness [m]}, respectively. The aerodynamic roughness depends on the surface status at target point. We adopt 0.3 m for grasslands. The height is not the geometrical elevation; it is length for vertical direction from the ground.

Even if the wind field is 4D, interpolation for time-axis is not calculated. But, when locations of dusts are moved by a wind of 10 min, a half interval (5 min) is used.

2.3 Difference expression div- and rot-operators

To get the divergence at (x,y)-point, we calculate $\{xi,yi\}$ set along a circumference of radius R [km], whose center is (x,y). The suffix "i" is angle [deg] from a reference axis (here, y-axis); the north direction is 0 [deg], and right rotation is positive.

The operation $\partial/\partial x$ for a value $V(x)$ is expressed as,

$\partial V/\partial x=\{V(x_i)-V(x_{-i})\}/(x_i-x_{-i}),$ (6)

Where the minus suffix "$-i$" is a symmetric point as for the center. Eq.(6) requires values at 2 $\{xi,yi\}$ points. Two mirror symmetries for x- and y-axis restricts "i" into [0,90] deg. Observation winds are discrete values of 16-directions. Then, the i-suffix is reduced into {0, 22.5, 45, 67.5, 90} deg. The divergence is not quantities depending on directions; we average the 5-direction values. Difference divergence values depends on radius R, we adopt $R=0.5$ km. We try to escape from constraint of mesh; however, we introduce a constraint like the mesh unfortunately.

The rotation of the vector field is,

$Rot(V)=Rot(Vx,Vy,Vz)=\{(\partial Vz/\partial y-\partial Vy/\partial z), (\partial Vx/\partial z-\partial Vz/\partial x), \partial Vy/\partial x-\partial Vx/\partial y)\}=(Ax,Ay,Az)$. (7)

Considering the expression, the (Ax,Ay) elements include $\partial/\partial z$-operation. The processing has difficulty in acceptable precisions. The Vz is calculated from $div(V)=0$ in Eq.(2). We set $Rot(V)$ to $Rot(0,0,Vz)$, which is an approximation. The rotation means vortex-intensity around small spherical floating in the air. *That is*, the approximation equals to set a force of z-direction.

Here, we discuss programing for a z-wind. From Eq.(2), we get,

$\partial Vz/\partial z=-\{\partial Vx/\partial x+\partial Vy/\partial y\}$. (8)

Considering "i" points around the center of V, an expression is got,

$(Vzi-Vz)/\{Distance(Vzi,Vz)\}=-[(Vxi-Vx)/\{Distance(Vxi,Vx)\}+(Vyi-Vy)/\{Distance(Vyi,Vy)\}]$, (9)

The left term of Eq.(9) is an element of Az of Wq.(7), which is summarized by N "i" indexes.

$Az=-N^{-1}\Sigma_{(i)}[(Vxi-Vx)/\{Distance(Vxi,Vx)\}+(Vyi-Vy)/\{Distance(Vyi,Vy)\}]$, (10)

2.4 Test of interpolated 4D wind field

The wind field is tested in various conditions; (1) movements on a plain, (2) scattering in vertical direction, (3) flow out ratio from interpolation plain, (4) correlation coefficients for other observations.

2.4.1 Movements in a plain

We simulate dusts in a zone of east longitude [140.7, 141.1] deg and the north latitude [37.35, 37.75] deg. The zone is 31×39 km. Square mesh points of 62×90 are selected as examples in the zone, whose interval is 0.5 km. The average winds are calculated and are compared with those of observation winds. The 3168 comparisons are processed per 10 min from April 28, 0:00, 2017 until May 19, 23:50, 2017, JST (Japan Standard Time). A correlation map is got, and the correlation coefficient is calculated, whose coefficient of determination is about 0.98. Using the linear regression, we get a linear function that corrects interpolated wind to that of mesh points. Slope and bias values of the function indicate small O(-2) different from 1 and 0; but the correction should be processed. The O(-n) is nth power of 10.

2.4.2 Scattering in vertical direction

It is found that 2 small disorder for SO_2 and SPM (Suspended Particulate Matter, dusts under diameter 10μm) during afternoon of May 7, 2017 at Haramachi district of south Soma city in Fukushima. We calculate 12 hour back-trajectories of Gaussian puffs (virtual air mass) for the afternoon, whose time interval is per 10 min and the height is 10 m. The results are in Figure 1.

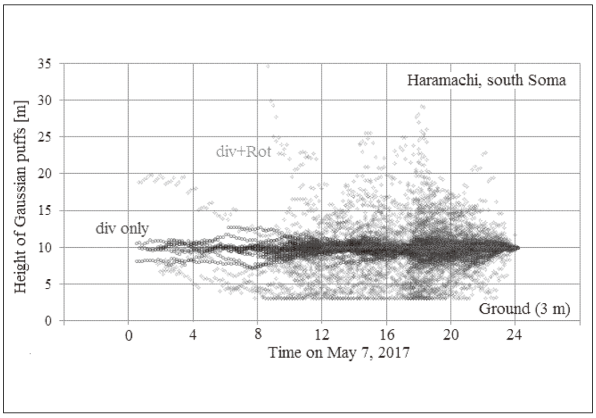

Figure 1. Distribution of back trajectory of Gaussian puffs.

Backward period is 12 h, each puff is started per 10 min, homogeneously. Height history of puffs is displayed by dots, in which the puffs are at Haramachi (south Soma, Fukushima), the time is May 7, 12:00 ~ 24:00, 2017 (JST). Blue dots are flown by the divergence and rotation, and red is by the divergence only. True color is referenced by Web-version.

We judge that the force of divergence only is not sufficient. Meteorological experimental indicates that the vertical wind-speed is about order of 1/100 for that of horizontal direction. The divergence force is less than the experiment; it would not be sufficient for turbulence. We can see the boundary (~18 h) between noon and night airs in blue distribution. Movement in the night is calm that fits Pasquill stability classes [9]. Moreover, reference Kondo [8] gives significant information.

2.4.3 Flow out ratio

The boundary condition in Eq.(1) is not set, it is open edge. There is no conservation law. We calculate probabilities flown out/in from the core area, whose east longitudes are [140.75, 141.10] deg, and the north latitudes are [37.35, 37.70] deg. It is gray and #9 zones in Figure 2. The counting period is between April 28, 0:00, 2017 and May 19, 23:50, per 10 min. We calculate movements after 10 min of a puff, which is repeated 15M.

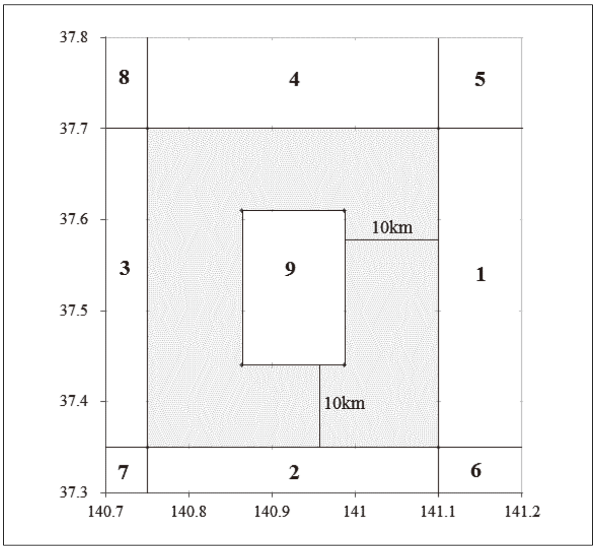

Figure 2. Divided areas to estimate probability of flow out/in puffs.
The outer 1 ~ 8 areas are infinity; their parts are drawn here.

Table 1. Moving ratios from the gray area

Area number	Ratio
1	7×10^{-3}
2	8×10^{-4}
3	8×10^{-4}
4	8×10^{-3}
5	1×10^{-4}
6	1×10^{-4}
7	0
8	1×10^{-4}
Existence gray	0.284
Go into 9	5×10^{-4}
Sub total	0.301
Stay in 9	0.699

Considering Table 1, the flow out probability is less than O(-2). It relates exchange of air against out areas. If the contribution is set to zero at the boundary, the error is O(-2). More suppressing the error, 5 observation points are added outside the area (see Appendix 1).

Another boundary for vertical is not considered; therefore, there is infinity area for the direction. In the paper, dusts are gradually fallen towards the ground, whose maximum height is given at the emission. The movements are in the surface layer; thus, the effect of no boundary is negligible.

2.4.4 Correlation coefficients

Ministry of environments of Japan has AEROS (Atmospheric Environmental Regional Observation System [10]). On some points, Yonomori, Shinzan, Odaka, Haramachi-1, winds per 1 h are observed. We compare calculated winds with those observations. These comparisons are listed in Figure 3.

The plotting wind is u-wind (east/west direction). The calculation is per 10 min, and the height is 10 m, and the values are converted to that of 1 h. The calculation includes both of interpolation and extrapolation. The determination coefficients are 0.66 ~ 0.79. They can be used as driving forces of dusts in the air, because of the indicator.

3. Emission of Dusts

3.1 Distribution of dust diameters

There is a little reliable information about radioactive dust floating around Fukushima accident point. MAFF measure monitoring results of atmospheric floating dusts and fallouts in Fukushima prefecture [11]. We find interesting data at Ottozawa and Shinzan, and Kiyohashi points. They are in Okuma and Futaba and Namie towns, and are located at 1.4, 4.2, 8.6 km distances from TEPCO Fukushima Daiichi nuclear power plant. The term is from June 25, 2014 to Aug 2, 2017, and the overlapped term is 917 days. The ^{137}Cs fallout masses are in Figure 4.

The sampling is done per a week. It is an interesting that much dust is falling suddenly. The event is displayed as a sharp peak. The 3 observation points are located along same direction; however, the peaks are not synchronized. It indicates the event is localized one; we believe the cause is strong gusts. We have tried to calculate the phenomenon; however, we could not get blast wind data on the district.

Average Cs-masses are 388.79, 19.57, and 8.71 [MBq/km^2] for Ottozawa, Shinzan, Kiyohashi. The ratio gives a distribution of the diameters of dust particles. The ratio is named; {r12, r23}={388.79/19.57=19.9,

19.57/8.71=2.3}. They are derived by solving the inverse problem under assuming diameter distribution functions; where the problem is reduced into parameter optimization of the functions. We adopt flowing functions,

$$D(r)=w_1 exp\{-A_1(r-c_1)^2\}+w_2 exp\{-A_2(r-c_2)^2\},$$

$$\int D(r)dr=1, \quad (11)$$

$$Gm(r)=wr^{\lambda} exp(-Ar^2),\ \int Gm(r)dr=1. \quad (12)$$

Both functions have plural parameters; Optimizing them, we reach a stationary point of Eq.(11). The derived ratio is {19.9, 2.24}, which is closed to {r12, r23}. The $\{w_1, w_2\}$ is {0.95694, 0.04306}, and $\{c_1, c_2\}$={80, 16.67} [μm], FWHM (full width half means)={80, 16.67}[μm]. Eq.(12) doesn't give a stationary point.

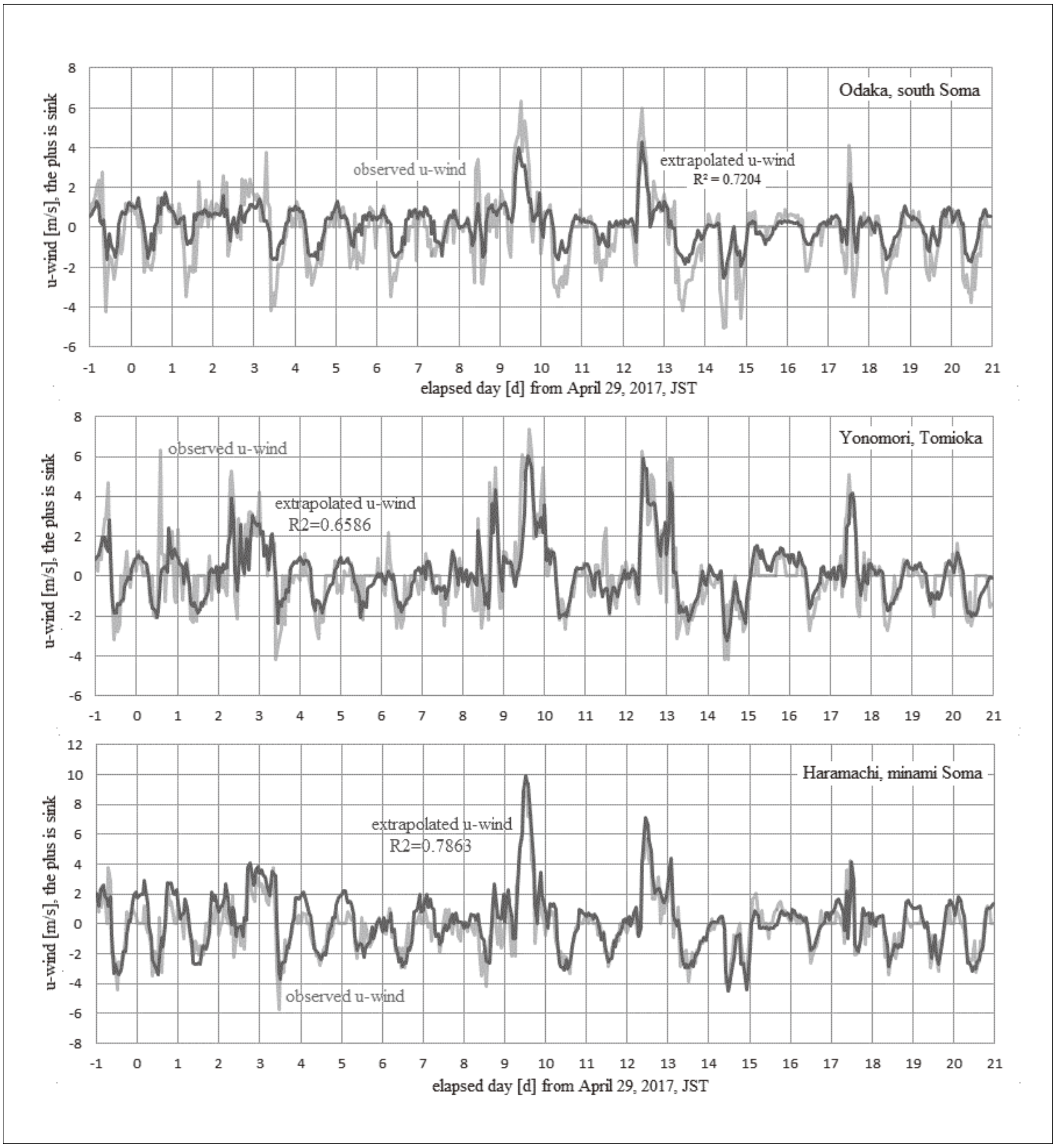

Figure 3. Comparisons with calculated winds (red) and observations (blue).

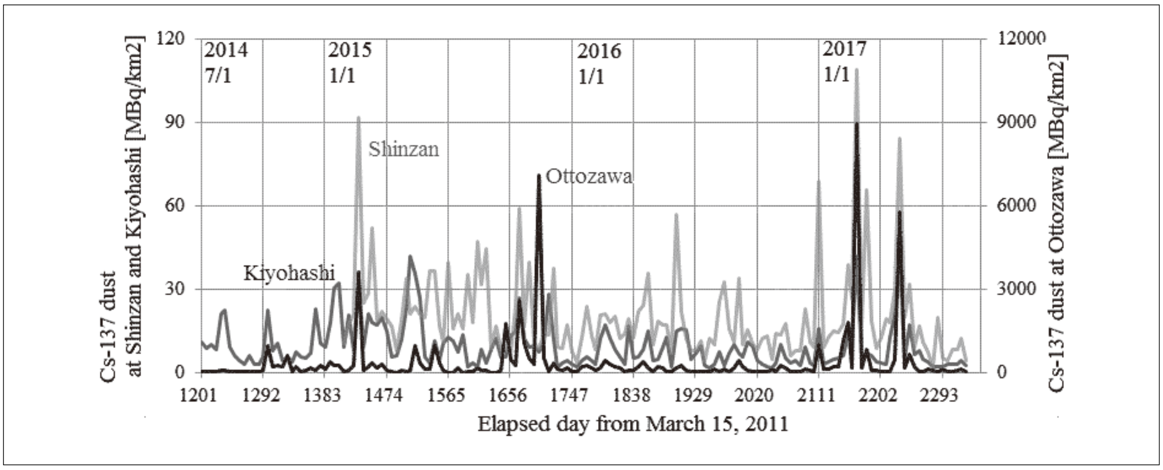

Figure 4. ^{137}Cs fallout masses at Ottozawa, Shinzan, and Kiyohashi points.

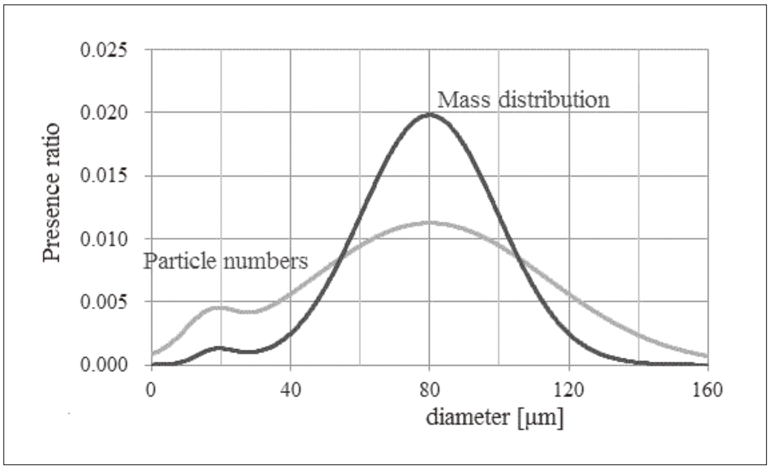

Figure 5. Diameter distribution of ^{137}Cs dust.
Blue line is for particle numbers, and red one is for mass of dusts. The ratio is calculated for integration=1.
Fallout mass relates the mass distribution. The distribution function is integrated in [0.001, 159.8] [μm] by numerical 4k points; we get 0.992. We get 4.93×10^{-4} and 1.70×10^{-2} in [0.001, 8.2] and [8.2, 26.1] [μm]. Therefore, radioactive Cs dust of 97.3% has diameters over 26.1 μm that is at the saddle point of red curve in Figure 5.

3.2 Terminal speed

The particle has terminal velocity under gravity and air property. The velocity $V(d)$ [cm/s] is classified by Reynold's number (Re), which is expressed,

$$V_1(d)=\{d^2(s-f)g\}/(18\mu),(Re < 2), \quad (13a)$$

$$V_2(d)=\{(4/225)(s-f)^2g^2/(f\mu)\}^{1/3}d,(2 < Re < 500), \quad (13b)$$

$$V_3(d)=[\{4/(3\times0.44)\}(s-f)gd/f]^{1/2},(500 < Re < 10^5), \quad (13c)$$

$$V(d)=\min\{V_1(d), V_2(d), V_3(d)\}. \quad (13d)$$

Where, $\{d, s, f, g, \mu\}$ is {diameter [cm], particle density [g/cm^3], air density [g/cm^3], gravitational acceleration [cm/s^2], viscosity of air [g/(cm×s)]}. We set $\{s, f, g, \mu\}=\{2.2, 0.001293, 980.665, 1.82\times10^{-4}\}$.

Using Eq.(13d) and considering major radioactive Cs dust over 26.1μm, they fall downward 100m in 0.75 h (see Appendix 2). At Iitate in Fukushima, radioactive dust is detected on wind speed over 3.3 m/s (see ref. [12]). Blowing up dust, and keeping the wind speed in 1 h; the reach distance is 8.9 km. Since such a condition is rare happened (see Figure 3), we consider small particle dust under 26.1 μm. Characters of dust including radionuclide are listed in Appendix 2.

3.3 An approximation of the air

We discuss movements of atmosphere of diameter of 1 ~ 2 km and thickness of several tens of meters. A functional equation, expressed by $\varphi(t,x,y,z):=\boldsymbol{\varphi}$;

$$\partial\boldsymbol{\varphi}/\partial t=Dxy(\partial^2/\partial x^2+\partial^2/\partial y^2)\boldsymbol{\varphi}$$
$$+Dz(\partial^2/\partial z^2)\boldsymbol{\varphi}-Cxy(\partial/\partial x+\partial/\partial y)-Cz(\partial/\partial z)\boldsymbol{\varphi}, \quad (14)$$

is a simplified advection-diffusion equation. Where Dxy, Dz, Cxy, Cz are scalar coefficients (that is an approximation of the Navier-Stokes equation [13]). We express an approximate solution, which is expanded by following functions;

$$h(t,x,y,z,\boldsymbol{k})=Nxy(t,\boldsymbol{k})Nz(t,\boldsymbol{k})exp[-Axy(t,\boldsymbol{k})\{(x-px(t,\boldsymbol{k}))^2$$
$$+(y-py(t,\boldsymbol{k}))^2\}]exp[-Az(t,\boldsymbol{k})\{z-pz(t,\boldsymbol{k})\}^2],$$
$$\varphi(t,x,y,z)=\Sigma_k\, h(t,x,y,z,\boldsymbol{k}), \quad (15)$$

The "$\boldsymbol{k}$" index is the attribution of mass that expresses the height of target atmosphere, dust's diameter, the specific gravity, and etc. Since they depend on each other, we write $\boldsymbol{k}$ as a generic index. We adopt atmosphere per attributions of mass (*cf.* Eq.(15)). We call it Gaussian-puff. To simplify suffixes, we eliminate "$\boldsymbol{k}$", hereafter.

Considering the conservation law, Eq.(15) is,

$$\int_\infty \varphi(t,x,y,z)dxdydz=\Sigma_k \int_\infty h(t,x,y,z,\boldsymbol{k})dxdydz. \quad (15a)$$

It is very difficult to introduce the law in simulation. We simulate under an assumption that density of the dust atmosphere is negligible small, and k of Σ_k is under several ten. The density is ppm-order in air environments (the error is under O(-4)).

The Gaussian-puff has a center, $\{px(t),py(t),pz(t)\}$, at time "t". $\{px(t),py(t),pz(t)\}=$

$$\{u(t_{0.5})t+px_0,\ v(t_{0.5})t+py_0,\ w'(t_{0.5})t+pz_0\}, \quad (16)$$

The location $\{px(t),py(t),pz(t)\}$ is calculated per an interval $[0,t]$. $\{u(t),v(t)\}$ is horizontal and vertical elements of the winds, which are interpolated. The z-element $\{w(t)\}$ is calculated from $div()=0$ and $Rot()$ in section 2.3. It is z-axis movements of pure air. That of the atmosphere including dusts is added by moving elements of the dusts. It depends on diameters of dusts. The terminal speed in section 3.2 is defined in calm air. In actual environments, small particles are not fallen, whose diameter is under 10 µm. It is found experimentally. The turbulence mixing force is existed in the air. We introduce a small constant (scalar) as a bias term.

$$w'(t)= w(t)+V(d)+bias. \quad (17)$$

Therefore, Eq.(17) cannot be applied for particles under diameter 10 µm. If the restriction is neglected, the particle's air would be diffused into higher layers.

The calculation is done by step by step. Plural steps make a trace, which has a distance. We write it u_{sum}. It relates A-parameters; which is derived by experiments for the atmosphere [9].

$$Axy(t)=1/\{2\sigma xy^2(t)\},$$
$$\sigma xy(t)=0.1107\{u_{\mathrm{sum}}(t_{0.5})t^{0.929}\},\ u(t_{0.5}) < 1\ [\mathrm{km}],$$
$$\sigma xy(t)=0.1467\{u_{sum}(t_{0.5})t^{0.889}\},\ u(t_{0.5}) > 1\ [\mathrm{km}], \quad (18)$$
$$Az(t)=1/\{2\sigma z^2(t)\},$$
$$\sigma z(t)=0.1046\{u_{sum}(t_{0.5})t^{0.826}\},\ u(t_{0.5}) < 1\ [\mathrm{km}],$$
$$\sigma z(t)=0.400\{u_{sum}(t_{0.5})t^{0.632}\},\ u(t_{0.5}) < 10\ [\mathrm{km}],$$
$$\sigma z(t)=0.811\{u_{sum}(t_{0.5})t^{0.555}\},\ u(t_{0.5}) > 10\ [\mathrm{km}], \quad (19)$$

Where "u_{sum}" equal to the distance moving from an origin point. The "$\sigma(t)$" includes many constants that are defined by measurements of atmosphere turbulence in middle stability day [9].

Characters of Gaussian are;

$$\sigma=(2A)^{-0.5},\ A=1/(2\sigma^2);\ N=\{\sigma(2\pi)^{0.5}\}^{-1},$$
$$FWHM=2\sigma\{2\ Ln(2)\}^{0.5},\ \textit{where suffix is omitted}, \quad (20)$$

"px_0" is location at $t=0$. The time is discrete one $\{t=0, 1, 2, ...\}$; but $t=0.5$ is defined as an exception. $FWHM$ is the full width half mean. By using Eq.(20) and Eq.(15), if emission rates of the dust are known at $t=0$, we calculate the density of Gaussian-puff at any point in the 4D space.

The approximation is derived from separate solutions of diffusion and advection parts. Therefore, the expression should not be applied over 100 steps (16.7 h). The formulation is defined in infinity space, thus; to calculate in finite space, we must discuss emission and annihilation of the puffs.

3.4 Expression of forest fire

We see a forest fire at Mt. Jyuman in Namie town, whose period is from 16:24, April 49, 2017 until 15:05, May 10, in which time is Japan standard time (JST) [14]. MAFF comments that ^{137}Cs of ~ 500 [kBq/m^2] is included in fallen leaf layers. Watching photography, the fire has no flame, and fallen leaves are burned. It would emit low calorie. Published news paper's photo is a fake (It is Canada's one). We conclude that ash is diffused into the air, and simulate the movement and deposition.

In environments contaminated by radioactive nuclides, a forest fire diffuses radioactive dust. The phenomenon is found at Chernobyl [15]. We have seen two forest fires in Fukushima, which are Reizan in Date-city and Mt. Jyuman in Namie-town. The periods are 4 and 12 days, respectively. About the Reizan fire, ISET-R (Interdisciplinary Study for Environmental Transfer of Radionuclides from the Fukushima Daiichi NPP accident) researches ^{137}Cs in the air by using high volume samplers. The detection mass is under 1×10^{-5} [Bq/m^3] [16]. As for Mt. Jyuman, Fukushima local government observes ^{137}Cs of maximum 2.5×10^{-2} [Bq/m^3] on Ishikuma point in Futaba-town, at May 12, 10:57 ~ 14:29, 2017, JST. Like observations are done at Yasuragi-Sou and Nogami-1ku points, and the period is from May 1, 14:14 to May 17, 14:22, 2017 [1]. They are important facts.

We see many news reports about the forest fire at Mt. Jyuman; but a little information for modeling re-diffusion of the forest fire. Following information is significant.

(1) MAFF's map of the burned area [1], (2) Findings of burned forest and their litter layers [1], (3) The fire fighting parties' comments from April 29, 16:24, 2017 to May 10, 15:05, 2017 [1]. (4) Volatilization temperature (> 1100 Celsius degree) of ^{137}Cs in the soil [17].

Judging them; the fire line is in fallen leaf layer and low calorific; and it exhausts a lot of smoke dust in case of strong winds. We consider a comment "The forest fire was almost extinguished on May 6 [14]. On May 7, the Mayor Namie's visit was planned." We construct a model for schedule of the forest fire. We estimate that the fire line is stopped at May 5, 18:00.

We consider that the forest fire can be divided into plural elemental phenomena. They are wind speed (*wS*), rainfalls (*rain*), virtual disk (radius R and area S). They are interacted with each other. The interaction is a forest fire model, which is stepwise processing. The wS is maximum wind speed during 3 s at the fire point. However; it is not observed. As a wind of same property, we adopt wind measured on a mountain (671m) at Tamura city [18]. The virtual disk is expressed by,

$$R(t)=R(t-1)+\delta R,\ \delta R=1/144, \quad (21)$$
$$S(t)=R(t)^2\{1-rain(t)F_3\},\ F_3=2^{0.5}/100,\ R(t)=S(t)^{0.5}, \quad (22)$$

The fire line is assumed as a circle, whose radius is expanded every day until May 5, 18:00. The circle area is decreased by the rainfall. The radius is recalculated by the area. The area correspond the burned area that is covered by ash. Thus; the product of the area and wS over 3.3 m/s is the ash flied into air. The threshold is observed for flying ground dusts at Tsushima district [19]. Blowing off ash would be near 2 values process. We adopt a continuous sigmoid function for the process. Continuous character is necessary to built-in a simulation. Knowledge of [20] is used for parameterization of the sigmoid function.

$Sw(t)=S(t)F_5\ Sigmoid\{wS(t)\}$,

$F_5=(37)^{-1}$, $Sigmoid(x)=[1+exp\{-5(x-6)\}]^{-1}$. (23)

The 3 constants, {37,5,6}, are got by fitting wind-speed characters found at Tsushima district [17], and by the normalization of [0, 1]. The $Sw(t)$ gives an emission ratio function that is in Figure 6. The ratio is emission rate. It can be used for multiply factor to Gaussian- puff density.

The absolute mass of the dust is unknown. It is derived by comparing observed dust densities at target points with simulation ones. The detail comments in Appendix 5.

The function is a discrete vector. The values indicate a flying-possibility of ash. The forest fire is terminated at May 10, 15:05, 2017; however, the flying-possibility of dust is not zero soon. The fallen leaf structures are destroyed by the fire, and after several rains, until new a structure are recovered, the possibility is not zero.

3.5 Deposition of dusts

The z-axis distribution is unknown about dust flied by instantaneous winds. There is no observation really. Estimating from field photos of the forest fire, smokes are in the surface layer. We believe the dusts exist between 10 ~ 120 m, and the density is larger for lower air layers. We adopt "E12" series that is expressed,

$\{zi;\ i=0,1,\ldots m\}=\{i\times Ln(10)/n;\ i=0,1,\ldots m\}$,

where $n=12$, $m\neq n$. (24)

It is a rational way to divide the length of 10 by n, when the dividing process has random errors. The $\{10\times zi;\ i=0,\ldots 13\}$ is Gaussian-puff's height [m] at $t=0$. The center is, $\{px(t),py(t),pz(t)\}=\{$*Eastern longitude, North latitude of the dust scattering point,* $10\times zi\}$. (25)

The Gaussian puff's half-mean width is $FWHM(t)$ at t, and 1 layer. When next condition is satisfied,

$pz(t)-FWHM(t)/2 < 0$, (26)

we define that the puff is attached on the ground. The puff is eliminated from a simulation of the advection-diffusion equation. Simulation of puffs in other layers is continued. We believe that ^{137}Cs migration ratio from the air to the ground surface is 1. Because, the deposition is observed by high volume samplers.

3.6 Back-trajectory Analyses

We separate the advection and diffusion equation to 2 parts, and solve it independently. If the diffusion part has a negligible effect for the solution, the equation has advection term only. The advection term is symmetric for inversion of the time. We write Eq.(16) as followings;

$\{px(t_{-1}),py(t_{-1}),pz(t_{-1})\}=$

$\{-u(t_{-0.5})t_{-1}+px_0,\ -v(t_{-0.5})t_{-1}+py_0,\ -w'(t_{-0.5})t_{-1}+pz_0\}$, (27)

The location $\{px(t_{-1}),py(t_{-1}),pz(t_{-1})\}$ is calculated per an interval $[t_{-1},0]$. Going back in time, the distribution of Gaussian centers is enlarged. If there is a significant contamination in air, its source is estimated by the backward simulation.

4. Simulation of a forest fire at Namie

4.1 YasuragiSou point

We simulate ^{137}Cs density in the air and deposition mass at YasuragiSou (Namie), Ishikuma (Futaba), and Nogami-1ku (Okuma). The GPS coordinates are listed in Appendix 3. The simulations are from April 30, 0:00, 2017 to May 19,

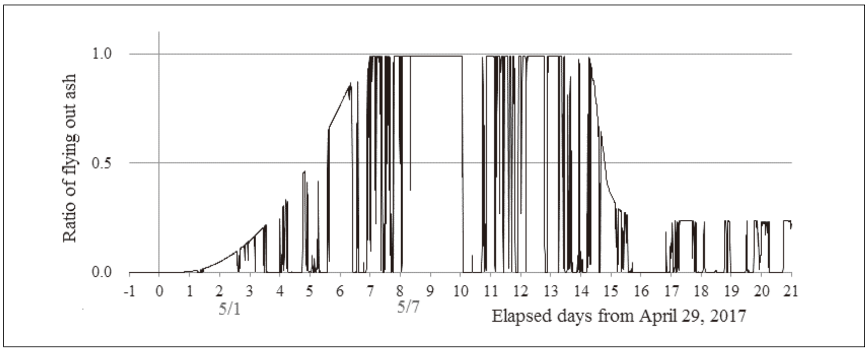

Figure 6. Emission ratio function for ash of Namie forest fire.

23:50 (JST), and the time interval is 10 min. The maximum of dusts mass in one air-layer is 1 at $t=0$, which is multiplied by the emission ratio function in section 3.4. It has the unit of [Bq/m^3]; however, the absolute value is unknown. We define it as 1, and simulate the deposition mass [Bq/m^2] of any point in 31×39 km plain (*cf.* section 1). If the deposition mass is observed; then we can estimate an exhaust radioactive mass at forest fire point. It gives a scale of transportation of radionuclides through the air.

The simulation is following conditions; (1) Emission locations are 11 points (Appendix 4). Layers of the air are 14, from 10 m until 121 m. (2) The distribution of radionuclides particles is 8.254 ~ 31.623 μm (E12 series divided by 8). (3) If the puffs reach the rain in 1 h from the start time, the puffs are eliminated. The rain is that of Namie AMDS (10 min). (4) Gaussian puffs are flied for 16 h, if they are not out of 31×39 km simulation area, or they are not deposited.

In the Figure 7, the origin of horizontal axis is April 29, 0:00, 2017 (JST). The axis is scaled by elapsed day [d]. The forest fire is between scale 0.7 and 11.6. Radionuclides are re-diffused after the fire. ^{137}Cs density of AIR graph indicates that of passing through on the point; green line does not correspond with blue bars. They are not detected density.

Deposition mass of GND graph corresponds with blue bars. The simulation indicates that ^{137}Cs is deposited in intermediate periods. Comparing the scales at both ends in Figure 7, we get,

4 mBq/m^3 : 7×10^{-9} =X:1; X=(4/7)×10^6 Bq/m^3.

Since there are 14 air-layers and 11 emission points (Appendix 4), X=3.7×10^3 Bq/m^3. From section 3.4, the density on the ground surface is 5×10^5 Bq/m^2. Therefore; radionuclides of 7.4% on the ground flies in the air per 1 d. This is the instantaneous maximum value. The estimation shows fire fighting parties need dust masks.

4.2 Levoglucosan

The Levoglucosan is in the tar obtained on pyrolysis of cellulose, whose temperature is between 300 ~ 550 [deg] Celsius temperature [19]. The yield is the maximum at 450

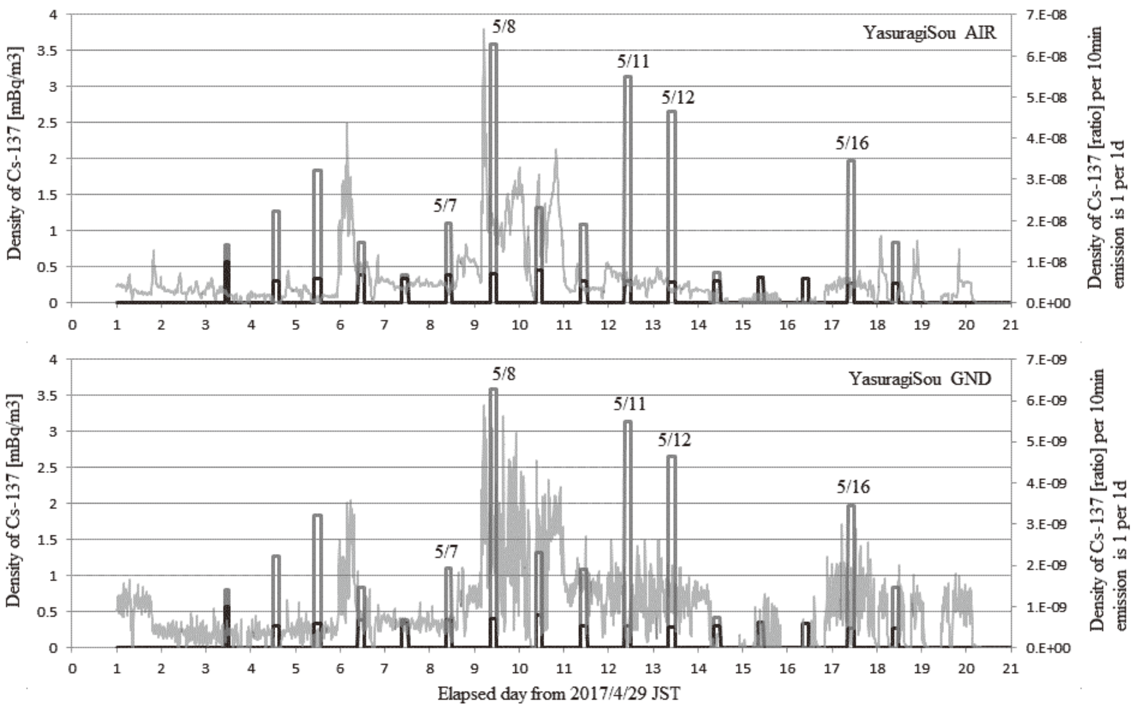

Figure 7. ^{137}Cs density in the air and deposition mass (GND) at YasuragiSou in Namie town.
Green zigzag lines indicate ^{137}Cs density (AIR graph) and deposition mass (GND graph). Bar graphs of blue and red are observation density and detection limits of high volume samplers. The observation is intermittent, and gives section data. There is no information among observations.

deg at normal pressure. Even if it is low caloric fire, the compound is diffused in the air. M. Ohara et. al. [20] measures it from May 1 to May 17, 2017. The paper will be published. Referencing ISET-R private communications, Levoglucosan is detected strongly from May 3 to May 9, at YasuragiSou point. The maximum peak is seemed to be May 6. Referencing green zig zag line in Figure 7, a Plume from the forest fire passes on the point at May 6. Main dusty plume passes after that day; we believe that Levoglucosan is evaporated soon by the heat.

4.3 Ishikuma point

The simulation at Ishikuma point gives Figure 8.

Flying radionuclides are about 10 times bigger than that of YasuragiSou point. The simulation indicates rather small peak values, oppositely, and gives continuous dust densities. Two large peaks of May 11 and 12 would be arisen by other physical mechanisms that are not included in the simulation.

4.4 Back trajectory

We calculate a back trajectory simulation, whose origin point is Ishikuma, and the time is from May 12, 11:00 ~ 15:00, and the backward period is 2 h. The trajectory passes near the west gate of Fukushima Daiichi nuclear power plant.

Simply considering a source of the peak, it would be a dismantling work of the decommissioning furnace. But, the prediction is denied by the fallout observation at Ottozawa point that is 1.4 km south direction of the furnace. Nowadays, the cause is not solved.

4.5 Deposition maps

Dusts flying from May 10 to 13, we calculate what happened to the dust that passed on Ishikuma point. It is main diffusions of the forest fire. To compress CPU, the simulation time is 6.5 h. The flying period calculates the density until relative dilution 1×10^{-14}. The deposition map is in Figure 10.

At Ishikuma point, radionuclides of 10 times are deposited in this period, from comparing with YasuragiSou. The order of mass is “Ishikuma > YasuragiSou > Nogami-

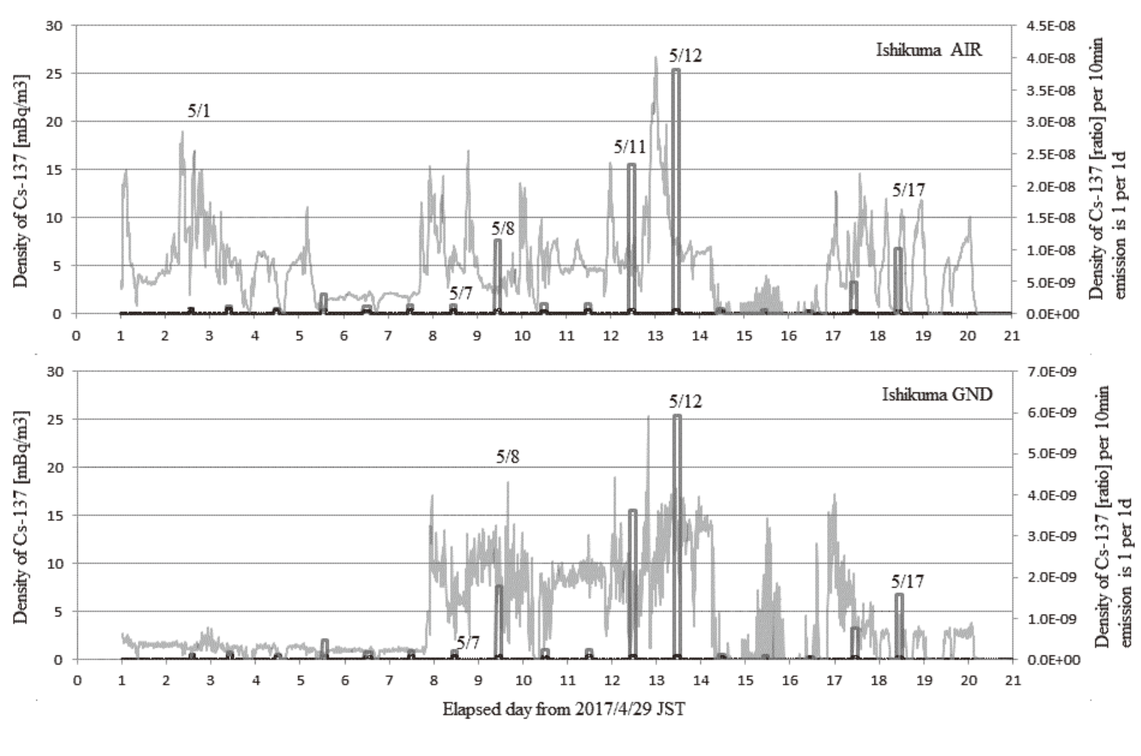

Figure 8. ^{137}Cs density in the air and deposition mass (GND) at Ishikuma point in Futaba town.
Green zigzag lines indicate ^{137}Cs density (AIR graph) and deposition mass (GND graph). Bar graphs of blue and red are observation density and detection limits of high volume samplers.

1ku", which is close to observations.

Dusts over through the 3 points are deposited on the ground in final; but they don't reach to other observation points set by Ministry of the Environment and Fukushima local government. Re-diffusion area is in Abukuma mountains. A NGO group observes dusts at Mt. Tekura (611m); however, the measurement has not significant precision compared with those of governments.

It is different time when the maximum Levoglucosan is detected and that of dusts. They are May 6, and May 8 at YasuraguSou point. Since we have no property data of Levoglucosan, we simulate dusts of the former/later days at May 7. Their deposition maps are in Figure 11/12. Since the contour lines are less than Figure 10, we write them by

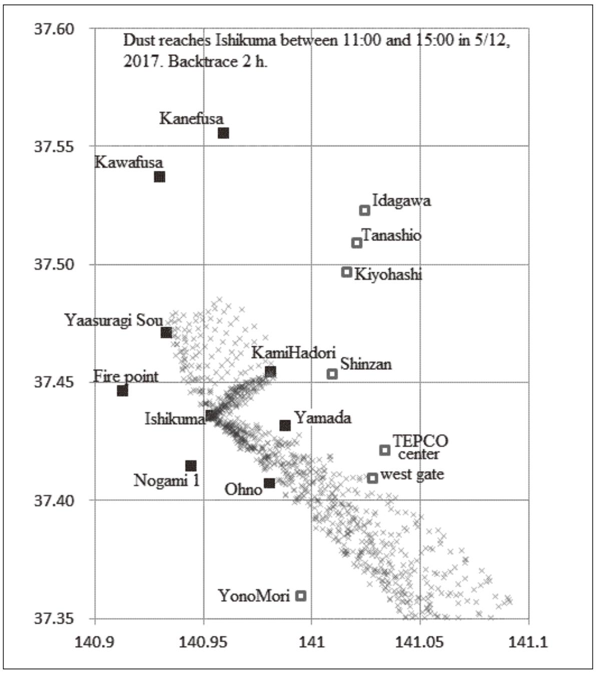

Figure 9. 2 hour back-trajectory of peak of May 12 at Ishikuma point.

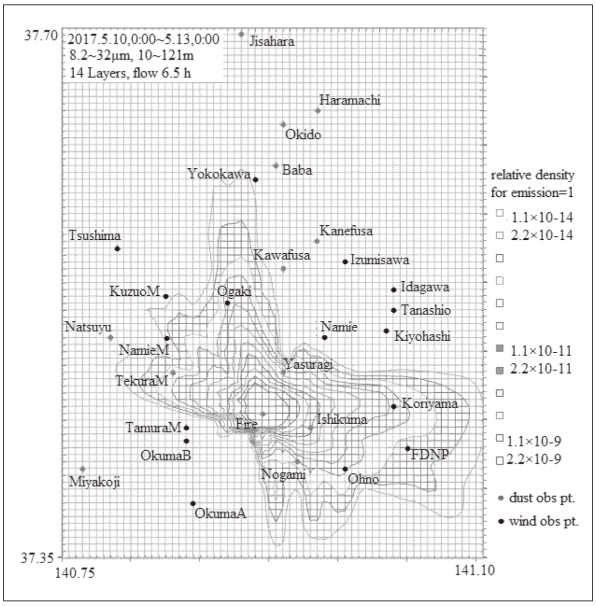

Figure 10. Deposition amounts [relative intensity] of radionuclides exhausted from a forest fire at Namie town, in the period from May 10, 0:00 to 13, 0:00, 2017, JST.

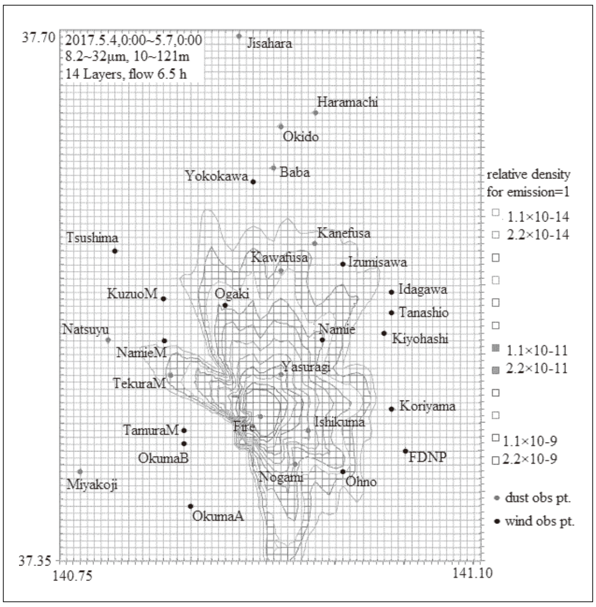

Figure 11. Deposition amounts [relative intensity] of radionuclides exhausted from a forest fire at Namie town, in the period from May 4, 0:00 to 7, 0:00, 2017, JST.

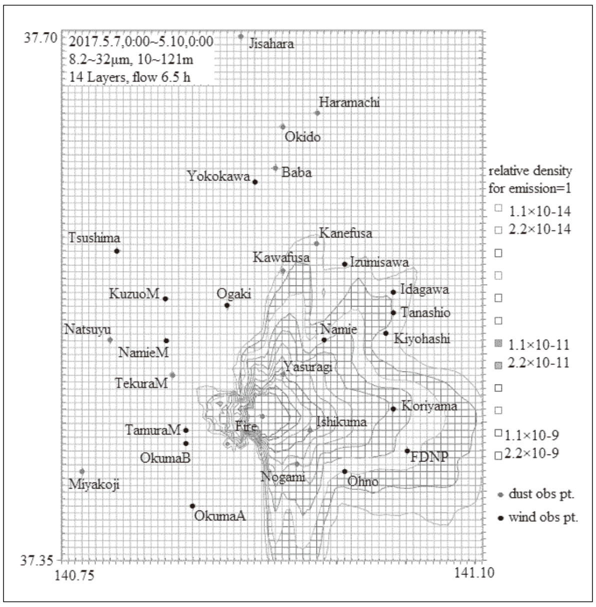

Figure 12. Deposition amounts [relative intensity] of radionuclides exhausted from a forest fire at Namie town, in the period from May 7, 0:00 to 10, 0:00, 2017, JST.

half-intervals of Figure 10.

The maximum Levoglucosan is detected in the period. Levoglucosan is transported for north direction from the fire point. Dr. Ohara shows YasuragiSou > Ishikuma as Levoglucosan. But, ^{137}Cs dusts show Ishikuma (3.60 mBq/m^3) > YasuragiSou (3.05 mBq/m^3), whose difference is small. “()” is the sum between May 4 and 6, where those of non-measurement period are neglected.

Levoglucosan is flowed towards east direction in the period, and detection amount shows YasuragiSou ~ Ishikuma. ^{137}Cs dusts show Ishikuma (9.50 mBq/m^3) > YasuragiSou (6.02 mBq/m^3). “()” is the sum between May 7 and 9, where those of non-measurement period are neglected.

4.6 Nogami 1-district point

The simulation at Nogami-1ku point gives Figure 13.

Deposition adionuclides are 1/2.3 of YasuragiSou point, and the simulation (GND) is 1/2.5. No detection between May 1 and May 6, and large peaks of May 8 and May 11 are emulated. The simulation is reasonable. There are plural strong peaks that are passed over the point, based on AIR-simulation; they are not detected.

4.7 Accumulations of depositions

We compare accumulated ^{137}Cs-density per 1 day. Here we execute a new simulation that gusts are taken into. The object is to revise small depositions at Ishikuma point. Strong wind blows large particles towards far points. The gust observations are a little in Fukushima unfortunately. By referencing Dr. Kondo [6], the probability of twice wind speed is 0.02275, where normal random process is assumed. The condition can be calculated easily.

The distribution of dust is expanded from 8.2 to 46.1 μm. Other situations are same. Considering random process, calculation results are compared with accumulated quantities. Since there is no dust-density measurement of 1

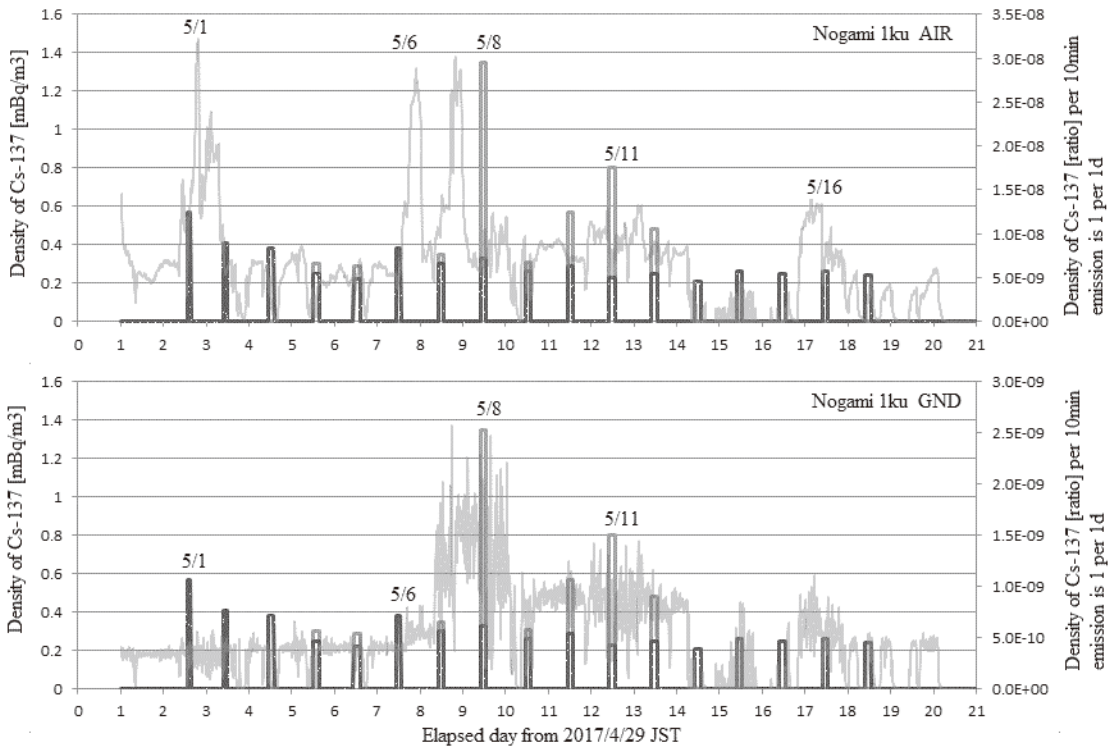

Figure 13. ^{137}Cs density in the air and deposition mass (GND) at Nogami-1ku district point in Okuma town.

Green zigzag lines indicate ^{137}Cs density (AIR graph) and deposition mass (GND graph). Bar graphs of blue and red are observation density and detection limits of high volume samplers.

day of Yasuragi Sou, Ishikuma, Nogami 1 ku points, we interpolate defects by using linear functions, and sum over the interpolations during 1 day. Simulated deposited ^{137}Cs-air quantities are also summed per 1 day. They are integrated in whole period, from April 29 to May 19; and fitted to the interpolations by multiplying factors. Factors of the 3 points are 1.02×10^{-10}, 1.48×10^{-11}, 1.09×10^{-10}. They are expected to be same values. Those of Yasuragi Sou and Nogami 1ku points satisfy the expectation; however, Ishikuma point is its 1/7. *That is*; some physical processes would not be taken account in the simulation.

Using simulation densities, observation ones, and inverse calculations, the density at fire points are 545, 3746, 511 kBq/m^3 per 1 day. The ^{137}Cs density in litter layers are 200~400 kBq/m^2 [11]. The simulation value is not reliable at Ishikuma point; it is abandoned. Other results equal to ^{137}Cs-concentration of 1 Layers. ^{137}Cs in a thin layer is blow off per 1 d.

Finding ^{137}Cs changes of Figure 14~16, the changes emulate interpolated observations. The simulation gives ^{137}Cs-accumulation map from May 1 until May 17 (Figure 17).

^{137}Cs density of Kawafusa point is 1/1000 of Yasuragi Sou point. Its amount is little; therefore, the detection would be difficult.

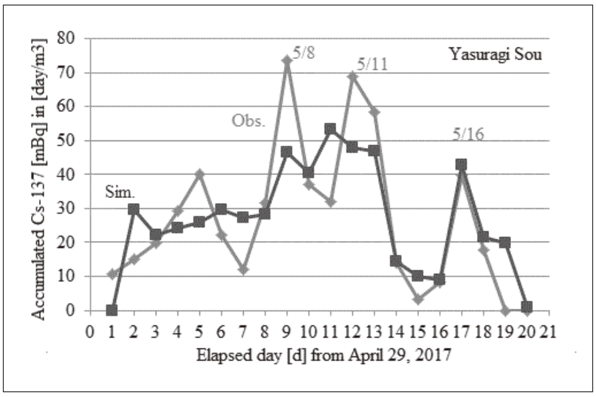

Figure 14. Changes of accumulated ^{137}Cs per 1 d, at Yasuragi Sou (Namie town).

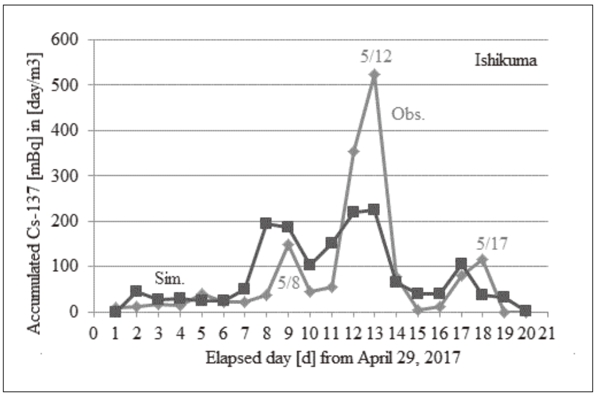

Figure 15. Changes of accumulated ^{137}Cs per 1 d, at Ishikuma point (Futaba town).

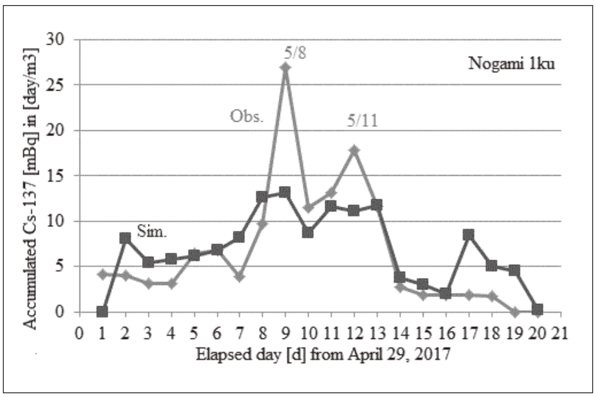

Figure 16. Changes of accumulated ^{137}Cs per 1 d, at Nogami 1ku point (Okuma town).

5. Conclusion

We show a construction method of 4D wind-field based on observations. The field is an useful tool for movement analysis of dusts or contaminants in the air. The applicable fields are restricted in the surface layer (< 120 m) of atmosphere, and no reaction event among contaminations. The field has no mesh structure; therefore, the precision of the convection equation is 16-bits.

We know a forest fire at Mt. Jyuman in Namie town; and find many exaggeration rumors in inter-net, which are arisen from less accurate knowledge. To correct the miss

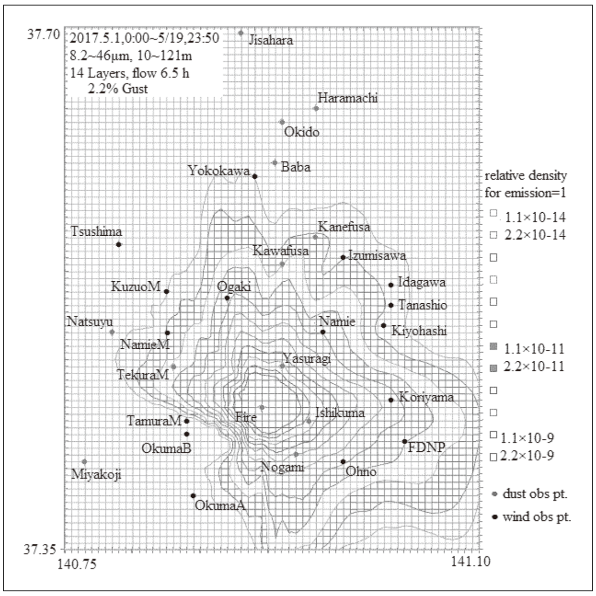

Figure 17. ^{137}Cs-deposition accumulated map from May 1 until May 17.

understands, we show a forest fire modeling. And we estimate status of dusts in the air, and simulate their movements and depositions. There may be insufficient point on our approaches; *i.e.*, the pulse events arisen by gusts is not calculated. We are wondering the event is not negligible for the two strong peak observed at Ishikuma point. However, the advanced processing must be started based on our basic simulation.

The dusts over through YasuraguSou, Ishikuma, and Nogami-1ku points are deposited on the ground in final. In forward tracing until 1×10^{-14} relative density, they don't reach to other observation points set by Ministry of the Environment and Fukushima local government. Re-diffusion area is in Abukuma mountains. Thus; we believe that the forest fire gives little effect to human living area.

Acknowledgement:

Contents of this paper are discussed at Sep. 5 in 2017, the 3rd work shop for information and education in University of Edogawa.

References

[1] Ministry of Agriculture, Forestry and Fisheries (MAFF), Forestry Agency, "Results of surveies on actual conditions of Namie and Futaba towns; the forest fire site in Fukushima Prefecture" ,
http://www.rinya.maff.go.jp/j/press/gyoumu/170623.html;
http://www.rinya.maff.go.jp/j/press/gyoumu/170623.html?cn=bWVzc2FnZQ%3D%3D

[2] GPV Data Archive in Japan is in Kitsuregawa laboratory in University of Tokyo; that is,
http://dias.tkl.iis.u-tokyo.ac.jp/gpv/ . The file name is,
Z__C_RJTD_YYYYMMDD000000_MSM_GPV_Rjp_Lsurf_FH00-15_grib2.bin, is 5.5km mesh data. They is formatted by Grib2.

[3] Japan Meteorological Agency, Meteorological DB (Japanese),
http://www.data.jma.go.jp/obd/stats/etrn/index.php. There are plural types data of the wind, in which the most important wind is that of 10 min. They cannot be got from the download page, but using cut & pastes display pages, they are got.

[4] Information of AMDS data; (1) To avoid effects by buildings, the wind is at 10 m on the ground. (2) The rainfall is counted per 0.5 mm. (3) There are points that have no wind measurements.

[5] Nuclear Regulation Authority, Monitoring information of environmental radioactivity level,
http://radioactivity.nsr.go.jp/map/ja/. Almost points have no wind measurements, but a few points have the wind data of 10min.

[6] Fukushima prefecture, monitoring department for radioactive rays,
https://www.pref.fukushima.lg.jp/sec/16025d/index-2.html.
Minami Soma City, division of civil living and environment section,
http://www.city.minamisoma.lg.jp/index.cfm/10,html.

[7] Inverse Distance Weighted (IDW) and Kriging,
http://desktop.arcgis.com/ja/arcmap/10.3/tools/3d-analyst-toolbox/how-idw-works.htm.
http://desktop.arcgis.com/ja/arcmap/10.3/tools/3d-analyst-toolbox/kriging.htm.

[8] J. Kondo," Chapter 1: Wind in the surface layer" ,
http://www.asahi-net.or.jp/~rk7j-kndu/kenkyu/ke01.html.

[9] Ministry of Environment, "Guidelines for waste disposal facility towards living environment"
https://www.env.go.jp/recycle/misc/facility_assess/mat02.pdf. There are many other guidelines (Japanese) by using PQ-diagram.

[10] Ministry of environments, AEROS,
http://soramame.taiki.go.jp/. The wind is measured per 1h. It cannot be used to construct with fields, but testing is enable.

[11] Ministry of Agriculture, Forestry and Fisheries, "Monitoring results of atmospheric floating dust and fallout in Fukushima prefecture (from August 20, 2014)" ,
http://www.maff.go.jp/j/kanbo/joho/saigai/fukusima/taiki/h26_8.html.

[12] As re-flying of dusts from the ground are studied in many cases.
(1) Y.Igarashi, "Approaches for Dust Transport by using Resuspension of ^{90}Sr and ^{137}Cs" , Japan Association of Aerosol Science and Technology, *Aerosol Kenkyu*, 17, pp. 252-258 (2002). ONLINE ISSN: 1881-543X, PRINT

ISSN: 0912-2834.
(2) K.Kita, et. al., "放射性物質の土壌と森林からの再飛散 (Re-diffusion the radioactive substances from the soil or the forest)" , Japan Society for Atmospheric Environment, 大気環境学会誌, Vol.49 (2014), No. 6, pp. A91-A92; http://doi.org/10.11298/taiki.49.A91.
On ref.(2); The radioactive dusts are detected from the wind speed 1 m/s at elevation 0.365m (friction speed), The speed corresponds with 3.3 m/s at 10 m height.

[13] Navier–Stokes equations, Wikipedia English, https://en.wikipedia.org/wiki/Navier%E2%80%93Stokes_equations.
The original expression is very difficult to calculate it numerically; therefore, differential parts for mass are omitted in this paper.

[14] Japan TV news24, http://www.news24.jp/articles/2017/05/07/07360814.html, published at May 7, 15:12, 2017.

[15] V.A KASHPAROVA, *et.al.*, "Forest fires in the territory contaminated as a result of the Chernobyl accident: radioactive aerosol resuspension and exposure of fire-fighters" , *Journal of Environmental Radioactivity*, Volume 51, Issue 3, pp. 281-298 (2000.12). The volume is a Special Issue for the Chernobyl accident.

[16] Private communications (emails) among ISET-R group. The contents are almost observations.

[17] K.Honma, et.al., "Removal of Cs from the Soil Contaminated with Radioactive Materials by heart treatment" , *The Clay Science society of Japan*, 52, pp.71-73 (2014).

[18] The data is offered from Japan Wind Engineering Co. Ltd. The GPS is #18 in Appendix 1.

[19] M.Miura, *et.al.*, "The pyrolysis of cellulosic materials and the analysis of levoglucosan in the tar" , *Report of the government industrial development laboratory, Hokkaido*, vol.35, pp.30-36, (1985.3), ISBN 0441-0734.

[20] Private communications (emails) among ISET-R group. The contents will be published.

Appendix 1. GPS of observation points for 10 min winds

#	Attr.	Point name	East longitude	North latitude
0	J	Namie AMDS	140.965	37.4917
1	N	Yokokawa Dam	140.908	37.5993
2	N	Oogaki Dam	140.884	37.5163
3	N	Ohno, Okuma	140.98	37.4067
4	N	Koriyama, Futaba	141.024	37.4481
5*	N	Tomioka	141.006	37.3411
6	N	Kiyohashi	141.016	37.4972
7	N	Izumisawa	140.984	37.5413
8	N	Natsuyu, Kuzuo	140.788	37.4936
9	N	UmaAraido, Miyakoji	140.765	37.4087
10	N	South Tsushima	140.798	37.5514
11*	J	Soma AMDS	140.925	37.78333
12*	N	ShimoKawauchi	140.8519	37.33707
13	T	West Gate, TEPCO	141.0336	37.42139
14*	J	Iitate AMDS	140.7267	37.665
15	G	Idagawa, south Soma	141.0244	37.52323
16	G	Mt.point Kuzuo	140.8349	37.52003
17	G	Mt.point Namie	140.8353	37.49448
18	G	Mt.point Tamura	140.8504	37.43647
19	G	Okuma B point	140.8504	37.4244
20	G	Tanashio, Namie	141.0205	37.50959
21	G	Okuma A point	140.8594	37.38728
22*	G	Obama, Tomioka	141.0287	37.34574
23	L	Haramachi, south Soma	140.9574	37.64212
24	L	Kawafusa	140.9302	37.53707
25*	J	Kawauchi AMDS	140.8083	37.33667
26*	J	Funehiki AMDS	140.5767	37.435
27*	N	Shigeoka	140.9983	37.30057
28*	N	Kotaki Daira	140.9571	37.22101
29*	N	Ogawa, Iwaki	140.8573	37.13351
30*	N	Kawamae, Iwaki	140.7711	37.19975
31*	N	Kido Dam	140.9157	37.26994

J: DB for meteorological phenomena published by Japan Meteorological Agency.
N: DB for Radioactivity level published by Nuclear Regulation Authority, Japan.
G: RAW data of 30-57m wind furnished by Tokyo gas Co. ltd, and the cooperation Ltd.
L: Daily reports of south Soma city.
Number* points locate out of the area in section "2.4.3 Flow out ratio". They are set to improve interpolation precision of winds.

Appendix 2. Characters of dust including radionuclide.

Diameter μm	# ratio*	Mass ratio*	T_speed cm/s	120m fall time h
8.254	0.002402	1.934×10^{-4}	4.96×10^{-4}	7.46
10.00	0.002903	3.413×10^{-4}	9.58×10^{-4}	5.06
12.12	0.003502	5.990×10^{-4}	1.94×10^{-3}	3.45
14.68	0.004103	9.640×10^{-4}	3.94×10^{-3}	2.35
17.78	0.004499	1.270×10^{-3}	7.48×10^{-3}	1.60
21.54	0.004470	1.246×10^{-3}	1.24×10^{-2}	1.09
26.10	0.004191	1.027×10^{-3}	1.74×10^{-2}	0.749
31.62	0.004339	1.140×10^{-3}	2.32×10^{-2}	0.507
38.32	0.005317	2.097×10^{-3}	3.37×10^{-2}	0.343
46.42	0.006891	4.566×10^{-3}	5.94×10^{-2}	0.235
56.23	0.008800	9.506×10^{-3}	0.127	0.160
68.13	0.01057	1.648×10^{-2}	0.284	0.109
82.54	0.01121	1.963×10^{-2}	0.555	7.42×10^{-2}
100.0	0.009449	1.177×10^{-2}	0.841	5.06×10^{-2}
121.2	0.005394	2.189×10^{-3}	0.973	3.90×10^{-2}
146.8	0.001626	5.995×10^{-5}	0.990	3.22×10^{-2}

*These values are derived from dusts fallen at Ottozawa, Shinzan, Kiyohashi points.

Appendix 3. GPS coordinates of YasuragiSou, Ishikuma-, Nogami 1ku points.

Point name	East longitude	North latitude
YasuraguSou	140.9333	37.47075
Ishikuma	140.953988	37.43568
Nogami 1ku	140.94467	37.414508

Appendix 4. Emission locations of the forest fire in Mt. Jyuuman at Namie town.

point	East longitude	North latitude	comment	km	deg
Peak of Mt. Jyuman	140.916545	37.448884	448.0m	Origin	Origin
Burned area center	140.913091	37.446107	H point		
NW limit point	140.910044	37.452206	_q point		
SE limit	140.918627	37.440315	_r point	0.814	142.3
S limit	140.910988	37.441882	_s point	0.502	200.7
NE limit	140.9197	37.447709	_t point	0.619	73.2
E limit	140.919614	37.445324	A point		
South #2 limit	140.913391	37.440315	u point		
small peak	140.913348	37.443075	341m _point		
Ridge	140.917211	37.443007	314m v point		
Ridge	140.916867	37.449344	436m w point		
Ridge	140.911589	37.452989	313m x point		

Appendix 5. How to convert observations measured by [Bq/m^2] and [Bq/m^3].

The mass of radionuclides deposited on the ground is measured by [Bq/m^2], the density in the atmosphere is done by [Bq/m^3]. They must be corresponded in order to analyze of the radionuclides emission.

The air is defined by 14 layers of E12-series. The fire line is defined by a circle that radius R [m]. Radionuclides contamination in the circle is homogeneous density, Y [Bq/m^2]. Therefore; the volume of the air is $V=14\pi R^2$ [m^3]. The E12-series has physical height, 10 ~ 121m. However, the interval is not equal. We introduce virtual equal intervals H, and $V=14H\pi R^2$ is a physical expression.

The radionuclide density is, $\sigma\pi R^2 Y/14H:=D$ [Bq/m^3]. To simplify $D=\sigma' Y/14$. The "σ'" is the *migration coefficient* that move matters from the ground to the air. In the convection-diffusion simulation, the dust emission is D=1 at t=0. This is our definition. If there is M-points emitted locations, for each points, D=1/M.